

# Probing single-electron scattering through a non-Fermi liquid charge-Kondo device

Eran Sela,<sup>1</sup> David Goldhaber-Gordon,<sup>2,3</sup> A. Anthore,<sup>4,5</sup> F. Pierre,<sup>4</sup> and Yuval Oreg<sup>6</sup>

<sup>1</sup>Raymond and Beverly Sackler School of Physics and Astronomy, Tel-Aviv University, IL-69978 Tel Aviv, Israel

<sup>2</sup>Department of Physics, Stanford University, Stanford, CA 94305

<sup>3</sup>Stanford Institute for Materials and Energy Sciences,

SLAC National Accelerator Laboratory, Menlo Park, CA 94025

<sup>4</sup>Université Paris-Saclay, CNRS, Centre de Nanosciences et de Nanotechnologies (C2N), 91120 Palaiseau, France

<sup>5</sup>Université Paris Cité, CNRS, Centre de Nanosciences et de Nanotechnologies, F-91120, Palaiseau, France

<sup>6</sup>Department of Condensed Matter Physics, Weizmann Institute of Science, Rehovot, 76100, Israel

(Dated: February 7, 2023)

Among the exotic and yet unobserved features of multi-channel Kondo impurity models is their sub-unitary single electron scattering. In the two-channel Kondo model, for example, an incoming electron is fully scattered into a many-body excitation such that the single particle Green function vanishes. Here we propose to directly observe these features in a charge-Kondo device encapsulated in a Mach-Zehnder interferometer - within a device already studied in Ref. 1. We provide detailed predictions for the visibility and phase of the Aharonov-Bohm oscillations depending on the number of coupled channels and the asymmetry of their couplings.

*Introduction.* The conventional Kondo effect is described by a local Fermi liquid theory [2]. One of its manifestations is the scattering phase shift resulting in a Kondo resonance forming at the Fermi level. The multi-channel Kondo (MCK) model, however, is described by a non-Fermi liquid (NFL) theory [3], and even the scattering of an electron incident at the Fermi level is inelastic [4]: it cannot be described by a single particle scattering phase shift. For the specific and most dramatic case of two channels, the incoming electron scatters purely into a many-body excitation [5, 6] with no elastic scattering, which is often referred to as the unitarity paradox [7]. For three or more channels there is a finite (yet non-unitary) elastic scattering probability which tends to unity in the limit of a large number of channels [5]. Though quantum dot (QD) experiments have proved successful in verifying many predictions on electronic transport through Kondo impurities, a direct observation of the single electron scattering amplitude in NFL states has remained elusive.

An experimental proposal [8] to measure the NFL single electron scattering consists of embedding a spin-Kondo QD [9, 10] in one arm of an Aharonov-Bohm (AB) interferometer. In this geometry, half of the conductance is expected to be incoherent while the other half is coherent with a definite phase shift [8] since only one linear combination of the source and drain leads couples to the QD while the other remains free, described by a FL theory. Realizing this setup with the necessary control of all parameters has been attempted by one of the present authors, but it has proved challenging.

In this paper we propose a complementary approach for observing the single electron scattering amplitude and phase in the Kondo effect, using a multi-channel charge-Kondo system [11, 12] based on quantum Hall edge states, embedded in a Mach-Zehnder interferometer. This experimental configuration was recently de-

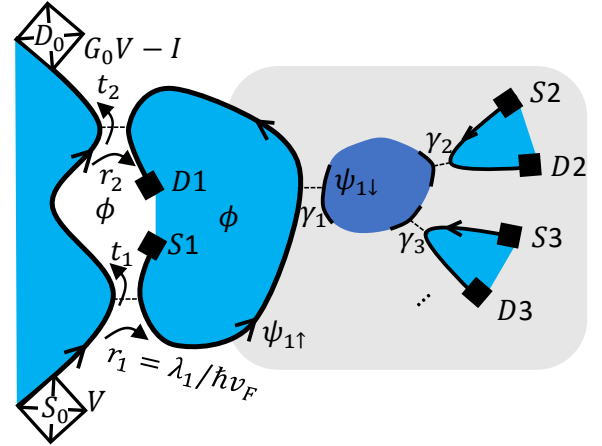


FIG. 1. Schematics of the device of Ref. 1 based on chiral edge states. The blue areas are in the  $\nu = 1$  quantum Hall state, with black boundaries denoting the propagating edge mode. The grey box including the dark blue confined dot highlights the Multi-channel Kondo system. The Mach Zehnder interferometer contains two QPCs with reflection amplitudes  $r_1$  and  $r_2$ . In the text we analyzed the differential conductance  $dI/dV$ .

signed by Duprez *et. al.* [1], see Fig. 1. Here, we argue that such a device is capable of directly identifying so-far-elusive information about the NFL nature of the MCK effect.

*Model.* The right hand side of the device in Fig. 1, demarcated by a gray box, is the charge-multichannel Kondo system. Recent experiments [11, 12] matched detailed conformal field theory predictions for the conductance of two and three channels:  $G_{2CK} = \frac{e^2}{2h}$  and  $G_{3CK} = \frac{4e^2}{3h} \sin^2 \frac{\pi}{5}$ , respectively, at the intermediate-coupling fixed points, as well as renormalization group flows toward the single channel fixed point as asymme-

try between the channels becomes apparent.

In this charge-based realization of the Kondo effect [13–15], two charge states of the QD play the role of the impurity spin: the  $N + 1$  charge state is mapped to “spin up”- and the  $N$  charge state to “spin down”. Consider weakly transmitting quantum point contacts (QPC) coupling the dot to the leads. Each reflection process in the QPC (i.e.  $\gamma_i$  in Fig. 1) translates into an impurity “spin flip”. To complete the analogy to spin, label the annihilation operators of spinless electrons in each lead ( $j = 1, 2, 3$  in the figure) by  $\psi_{j\uparrow}$ , and spinless electrons inside the QD near each QPC by  $\psi_{j\downarrow}$  as marked in Fig. 1. As the Kondo effect requires a continuum in both spin flavors, the electronic level spacing in the QD must be negligible. In practice, incorporating a metal (with its high density of states) into the QD has allowed achieving this criterion without making the charging energy unacceptably small.

Thus, the free part of the Hamiltonian  $H = H_0 + H_K$ , describes  $2_{QD/lead} \times 3_{QPCs}$  chiral channels,  $H_0 = \sum_{\alpha=\uparrow,\downarrow,j=1,2,3} \int dx \psi_{j\alpha}^\dagger(x) i v_F \partial_x \psi_{j\alpha}(x)$ . There is no elastic transport between different QPCs due to the large ratio between the temperature and the level spacing in the metallic QD [13–15]. The Kondo interaction simply describes tunneling in and out of the QD [16],

$$H_K = \sum_j \gamma_j \psi_{j\downarrow}^\dagger(0) \psi_{j\uparrow}(0) S^+ + h.c. + \Delta E S^z, \quad (1)$$

with amplitudes  $\gamma_j$ . Here  $S^+ = |N + 1\rangle\langle N|$ ,  $S^z = (|N + 1\rangle\langle N + 1| - |N\rangle\langle N|)/2$ , and  $\Delta E \propto V_g - V_g^0$  describes a gate-voltage-dependent energy splitting between the two charge states.

The MZ interferometer in Fig. 1 consists of two arms denoted 0 and 1. The zeroth (“reference”) arm in the left side in Fig. 1 is described by a chiral fermion  $H_{0,ref} = \int dx \psi_0^\dagger(x) i v_F \partial_x \psi_0(x)$ . Arm 1 is described by  $\psi_{1\uparrow}$ . The tunneling Hamiltonian of the MZ interferometer is

$$H_{tun} = \lambda_1 \psi_0^\dagger(-L) \psi_{1\uparrow}(-L) + \lambda_2 e^{i\phi} \psi_0^\dagger(L) \psi_{1\uparrow}(L) + H. \quad (2)$$

where  $\phi$  is the AB flux in units of  $h/e$ .

*Interference current.* Useful information about the MCK state can be extracted from the current within second order perturbation theory in the tunneling amplitudes  $\lambda_{1,2}$ . To leading order these are given in terms of the reflection amplitudes at the MZ QPCs,  $r_i = \lambda_i/(\hbar v_F)$  [17] ( $i = 1, 2$ ). In the absence of the QD ( $\gamma_1 = 0$ ), the conductance between arm 0 and arm 1

$$\left. \frac{dI}{dV} \right|_{\gamma_1=0} = \frac{e^2}{h} |r_1 + r_2 e^{i\phi}|^2. \quad (3)$$

The current can be separated as  $I = I_0 + I_\Phi$ , where  $I_0 \propto |r_1|^2 + |r_2|^2$  does not depend on the AB flux, and  $I_\Phi$  is the interference term, which in the absence of the QD ( $\gamma_1 = 0$ ) is  $dI_\Phi/dV = \frac{e^2}{h} (r_1 r_2^* e^{-i\phi} + h.c.)$ .

Calculating the current using the Kubo formula to second order in the reflection, one finds [1, 18]

$$I_\Phi = r_1 r_2^* e^{-i\phi} \int_{-\infty}^{\infty} dt e^{iVt} \times \quad (4)$$

$$(\langle \psi_0^\dagger(-L) \psi_0(L, t) \rangle \langle \psi_1(-L) \psi_1^\dagger(L, t) \rangle - \langle \psi_0(L, t) \psi_0^\dagger(-L) \rangle \langle \psi_1^\dagger(L, t) \psi_1(-L) \rangle) + h.c.$$

We see that the interference term probes the electron propagator between  $x = -L$  and  $x = L$ , which for arm 1 is sensitive to the scattering amplitude of the QD.

The interference term  $r_1 r_2^* e^{-i\phi}$  in Eq. (3) corresponds to an electron passing uninterrupted through channel 1, unaffected by the QD. This is obtained by substituting the free Green function denoted  $G_0$  for both arms [17]. In this case the variation of the conductance due to the AB oscillations is given by  $4|r_1 r_2|$ . The smallness of  $r_1$  and  $r_2$  guarantees that the interference term is due to a single electron being injected into arm 1. Practically, it is sufficient to demand that only  $|r_1| \ll 1$  whereas  $|r_2|$  can be of order unity.

All nonzero orders in the  $\gamma_j$ 's are encoded by the exact  $\mathcal{T}$ -matrix [19, 20],  $G(\omega, -L, L) = G_0(\omega, -L, L) + G_0(\omega, -L, 0) \mathcal{T}(\omega) G_0(\omega, 0, L)$ . Substituting into Eq. (4) yields at zero temperature [17, 21]

$$G_\Phi \equiv \frac{h}{e^2} \frac{dI_\Phi}{dV} = r_1 r_2^* e^{-i\phi} \mathcal{S}(eV) + h.c., \quad (5)$$

where

$$\mathcal{S}(\omega) = 1 - 2\pi i v \mathcal{T}(\omega). \quad (6)$$

As a matrix,  $\mathcal{S}$  is diagonal in both on-site pseudospin and channel index, and we refer throughout to the matrix elements  $\mathcal{S}_{1\uparrow,1\uparrow}$  as probed by the MZ interferometer (and similarly for  $\mathcal{T}$ ). Since this result is perturbative in the tunneling between arms 0 and 1, the voltage  $V$  sets the value of the frequency of the  $\mathcal{T}$  matrix computed at equilibrium.

From the  $\mathcal{S}$ -matrix, we see that the visibility, i.e. the difference in conductance in units of  $e^2/h$  between maximum and minimum, is given by  $4|r_1 r_2| |\mathcal{S}|$ , and the phase of the AB oscillations is given by  $\arg \mathcal{S}$ ,

$$G_\Phi(V, T) = 2|r_1 r_2| |\mathcal{S}(eV)| \cos(\arg(r_1 r_2^*) + \arg(\mathcal{S}(eV)) - \phi). \quad (7)$$

We refer to  $|\mathcal{S}|$  as the *relative visibility* with respect to the trivial case in Eq. (3).

Consider first the case where  $k$  QPCs are equally coupled ( $\gamma_1 = \gamma_2 = \dots = \gamma_k$ ), and where the gate voltage of the QD is tuned to an exact degeneracy between the two charge states ( $\Delta E = 0$ ). In this case we employ the Affleck and Ludwig result for the  $\mathcal{S}$ -matrix at the  $k$ -channel Kondo fixed point [5],

$$\mathcal{S}_k = \frac{\cos[2\pi/(2+k)]}{\cos[\pi/(2+k)]}, \quad (k \geq 2). \quad (8)$$

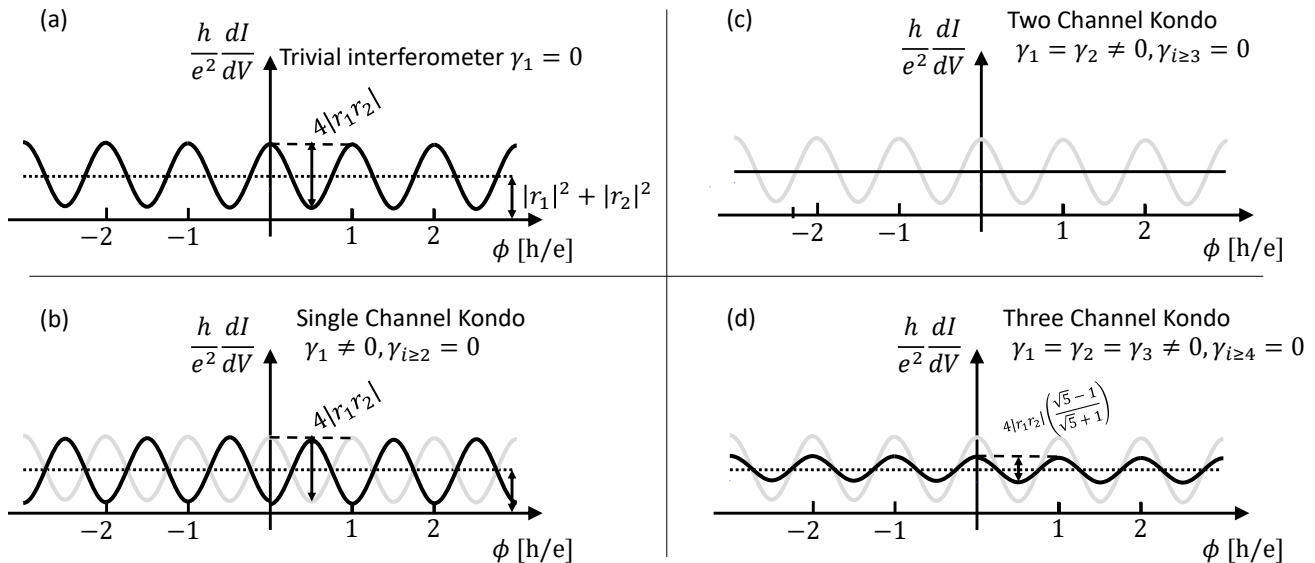


FIG. 2. AB oscillation patterns for (a) the trivial case with a detached QD, and for (b) 1CK, (c) 2CK and (d) 3CK configurations. Both the amplitude of the phase of the single electron scattering amplitude  $\mathcal{S}$  in the  $k$ -channel Kondo state can be read by comparison with the trivial reference case of (a).

We emphasize that this result with a real scattering amplitude (being  $\geq 0$  except for  $k = 1$  for which  $\mathcal{S}_1 = -1$ ) only holds at the charge degeneracy point,  $\Delta E = 0$ . Plugging this result into Eq. (7), in Fig. 2 we illustrate the conductance as a function of flux. In a reference configuration with the QD detached from the first arm ( $\gamma_1 = 0$ ),  $G_\Phi = r_1 r_2^* e^{-i\phi} + h.c.$ . Namely, the visibility is given by  $4|r_1 r_2|$  with an arbitrary phase dictated by details such as the interferometer length [Fig. 2(a)].

*1CK effect.* Connecting the QD only to the first arm, ( $\gamma_1 \neq 0, \gamma_2 = \gamma_3 = 0$ ), the 1CK effect develops. This is an example of a FL fixed point described in terms of a scattering phase shift  $\delta$ , such that  $\mathcal{S} = e^{2i\delta}$  is unitary. For the 1CK effect at the charge degeneracy point  $\Delta E = 0$ , corresponding to zero Zeeman field in the usual “spin” Kondo system,  $\delta = \pi/2$ , hence  $\mathcal{S} = e^{2i\delta} = -1$ . This leads to a unit relative visibility and a  $\pi$ -shift of the interference term, as in Fig. 2(b).

A finite gate detuning  $\Delta E \neq 0$  leads to a deviation of the average charge of the island from  $N + 1/2$ . As  $\Delta E$  varies, the charge of the QD  $N(\Delta E)$  displays Coulomb steps for small enough  $\gamma_i$ 's [15]. In a FL at  $T = 0$  the phase shift is directly related to the charge via the Friedel sum rule,  $\delta(\Delta E) = \pi N(\Delta E)$ . In an experiment, probing the phase via the MZ interference, while simultaneously capacitively measuring on-site charge would test that this sum rule holds. As the QPCs become more and more open (i.e. upon increasing the  $\gamma_i$ 's), the charge as a function of gate voltage should gradually increase with a constant slope up to weak Coulomb oscillations, as can be observed using these two measurements.

At  $T = 0$  the variation of the AB phase through the MZ interferometer upon varying the gate detuning  $\Delta E$  can be accounted for by a noninteracting scattering model. However, the key property that cannot be explained by a single-electron scattering model is the reduction of the visibility occurring in multichannel case.

*Symmetric MCK fixed points.* We proceed by coupling additional leads, but first setting the QD to charge degeneracy,  $\Delta E = 0$ . Upon coupling to the QD a second channel ( $\gamma_1 = \gamma_2 \neq 0, \gamma_3 = 0$ ), as in Fig. 2(c), the visibility vanishes,  $\mathcal{S}_{k=2} = 0$ , and thus the interference term completely disappears as  $T, V \rightarrow 0$ . In other words, in contrast to the previously-considered realization of the 2CK with a single electron quantum dot [8], here the unitary paradox of the 2CK NFL state [7] directly manifests in the visibility.

We note that the experimental results in Duprez *et al.* [1] are reminiscent of the sequence of behaviors in Fig. 2(a,b,c) although a different interpretation was given in a different regime with large  $r_{1,2}$ , uncontrolled  $\gamma_{1,2}$  and unknown energy splitting between pseudospin (charge) states.

Finally, upon coupling the QD to a third channel with equal magnitude ( $\gamma_1 = \gamma_2 = \gamma_3 \neq 0$ ) as in Fig. 2(d), the visibility approaches  $\mathcal{S}_{k=3} = \frac{\sqrt{5}-1}{\sqrt{5}+1} = 1 - 1/\varphi$  where  $\varphi$  is the golden ratio, with the phase shift reverting to its reference value. Observing all the different behaviours shown in Fig. 2 in a single device, as couplings are tuned, could not be explained by a noninteracting single electron model.

Below we discuss the effect of various symmetry break-

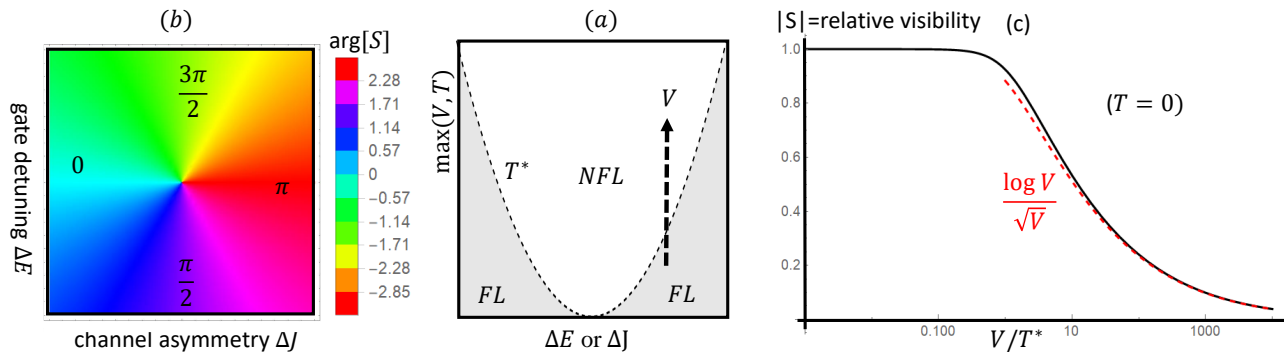


FIG. 3. (a) 2CK quantum critical point, displaying an energy scale  $T^*$  which vanishes at the critical point controlled by symmetry breaking perturbations  $\Delta J$  and  $\Delta E$ . (b) The AB phase  $\arg S$  changes continuously, winding by  $2\pi$ , as the NFL state is encircled in the plane spanned by  $\Delta J$  and  $\Delta E$ . (c) For  $T^* \ll T_K$  the crossover of the visibility (as well as phase shift, not shown), can be computed exactly, see Eq. (11).

ing perturbations such as channel asymmetry or gate voltage detuning.

*Symmetry breaking FL states.* We now consider the FL fixed points obtained by starting from the 2CK state  $\gamma_1 = \gamma_2$ ,  $\gamma_3 = 0$ , and either breaking the particle-hole symmetry by a gate voltage  $\Delta E \neq 0$ , corresponding to a Zeeman field on a conventional spin-based Kondo impurity, or by breaking the channel symmetry by a finite  $\Delta J = \gamma_1 - \gamma_2 \neq 0$ . Any small deviation from the “spin” and channel symmetries generates an energy scale  $T^*$ , such that upon lowering the temperature or voltage below  $T^*$ , the system undergoes a crossover from NFL to FL behavior [22–24], see Fig. 3(a). For the 2CK case the crossover scale is quadratic in the perturbations [16, 22, 25]

$$T^* = \eta_1^2 + \eta_2^2, \quad \eta_1 \propto \Delta J, \quad \eta_2 \propto \Delta E. \quad (9)$$

Manifestations of this FL-NFL crossover were studied experimentally both for spin-Kondo [24] and charge-Kondo systems [11], as well as in other devices [23].

We now consider the low energy limit,  $T, V \rightarrow 0$ . The phase shift in the FL regime depends on the ratio between channel anisotropy  $\Delta J$  and gate voltage detuning  $\Delta E$ . For  $\Delta E = 0$  the FL switches from a 1CK state occurring with channel 1 for  $\gamma_1 > \gamma_2$ , in which case  $\delta = \pi/2$ , to one occurring with channel 2 for  $\gamma_2 > \gamma_1$ , in which case  $\delta = 0$ . These two values of the phase shift correspond to the  $\Delta E = 0$  line in Fig. 3(b). It is interesting to explore the effect of encircling the NFL point  $\Delta E = \Delta J = 0$  [26]. As seen in Fig. 3(b), the phase shift performs a full winding by  $\pi$  (with the definition  $\mathcal{S} = e^{2i\delta}$ ) [22, 27, 28],

$$\mathcal{S}_{FL} = -\frac{\eta_1 + i\eta_2}{\sqrt{\eta_1^2 + \eta_2^2}}. \quad (10)$$

In the pseudospin-polarized FL state for dominating  $\Delta E$ , the phase shift is  $\pi/4$  or  $3\pi/4$  corresponding to a complex scattering amplitude  $e^{2i\delta} = \pm i$  [22]. Thus, the present MZ device can probe this phase shift winding around the NFL fixed point.

*Exact NFL-FL crossover.* Based on the phase diagram in Fig. 3(a), one expects that the relative visibility of the 2CK MZ device will depend on the energy scale. Setting  $T = 0$  for simplicity, we expect a NFL region for  $eV \gg T^*$  with vanishing visibility, and a FL region for  $eV \ll T^*$  with unit relative visibility. Interestingly, the 2CK model perturbed by any combination of channel asymmetry or Zeeman field maps to a known statistical mechanics problem known as the boundary Ising model [29] for which exact results are known [30]. Borrowing these results, the Green function in the presence of a finite perturbation  $T^*$  has been computed along each of these crossovers [27, 28]. The  $\mathcal{S}$ -matrix is given by

$$\mathcal{S} = \mathcal{S}_{FL} \mathcal{G}(\omega/T^*), \quad (11)$$

where  $\mathcal{G}(x) = \frac{2}{\pi} K[ix]$ ,  $K[x]$  is the complete elliptic integral of the first kind, yielding asymptotically  $\mathcal{G}(x) = 1 + ix/4 - (3x/8)^2 + \mathcal{O}(x^3)$  for  $x \ll 1$ ; and  $\mathcal{G}(x) = \frac{\sqrt{i}}{2\pi} (\log[256x^2] - i\pi)x^{-1/2}$  for  $x \gg 1$ .

Plugging the exact Green function into Eq. (7), we obtain the visibility and phase shift analytically. As shown in Fig. 3(c) the relative visibility given by  $|\mathcal{G}(eV/T^*)|$  tends to 1 in the FL regime and decays as  $1/\sqrt{V}$  for  $eV \gg T^*$  in the NFL regime. Due to the complex structure of the function  $\mathcal{G}(\omega/T^*)$  the phase of the AB oscillations,  $\arg(\mathcal{S}(eV))$  in Eq. (7) also displays a crossover as a function of  $V$  (not shown) as confirmed with NRG [28].

*Summary and outlook.* We analyzed an electronic Mach-Zehnder interferometer in the quantum Hall regime as a proposed setup to directly probe longstanding predictions on the scattering phase and sub-unitary scattering amplitude of single electrons in the multi-channel Kondo effect. The setup in general allows probing any quantum impurity model including multiple-impurity systems exhibiting exotic critical points as recently studied experimentally [31, 32]. An interesting future direction would be to use such an interferometer to probe the phase and possibly non-abelian statistics of Kondo

anyons [33–36] by placing multiple dots along the chiral interference arm.

*Acknowledgments.* ES, AA and FP acknowledge support from the European Research Council (ERC) under the European Unions Horizon 2020 research and innovation programme under grant agreement No. 951541. ES acknowledges ARO (W911NF-20-1-0013) and the Israel Science Foundation, grant number 154/19. YO Acknowledges support from the ERC under the European Union’s Horizon 2020 research and innovation programme (grant agreements LEGOTOP No. 788715), the DFG (CRC/Transregio 183, EI 519/7-1). DGG acknowledges support from U.S. Department of Energy, Office of Science, Basic Energy Sciences, Materials Sciences and Engineering Division, under contract DE-AC02-76SF00515, at the initiation of the project, and from the Gordon and Betty Moore Foundation’s EPIQS Initiative through grant GBMF9460 at later stages. We thank Christophe Mora and Dor Gabai for discussions.

- 
- [1] H Duprez, E Sivre, A Anthore, A Aassime, A Cavanna, U Gennser, and Frédéric Pierre, “Transmitting the quantum state of electrons across a metallic island with coulomb interaction,” *Science* **366**, 1243–1247 (2019).
- [2] Philippe Nozieres, “A “fermi-liquid” description of the kondo problem at low temperatures,” *Journal of low temperature physics* **17**, 31–42 (1974).
- [3] Ph Nozieres and Annie Blandin, “Kondo effect in real metals,” *Journal de Physique* **41**, 193–211 (1980).
- [4] László Borda, Lars Fritz, Natan Andrei, and Gergely Zaránd, “Theory of inelastic scattering from quantum impurities,” *Phys. Rev. B* **75**, 235112 (2007).
- [5] Ian Affleck and Andreas WW Ludwig, “Exact conformal-field-theory results on the multichannel kondo effect: Single-fermion green’s function, self-energy, and resistivity,” *Phys. Rev. B* **48**, 7297 (1993).
- [6] VJ Emery and S Kivelson, “Mapping of the two-channel kondo problem to a resonant-level model,” *Phys. Rev. B* **46**, 10812 (1992).
- [7] Juan M Maldacena and Andreas WW Ludwig, “Majorana fermions, exact mapping between quantum impurity fixed points with four bulk fermion species, and solution of the “unitarity puzzle,”” *Nuc. Phys. B* **506**, 565–588 (1997).
- [8] Assaf Carmi, Yuval Oreg, Micha Berkooz, and David Goldhaber-Gordon, “Transmission phase shifts of kondo impurities,” *Phys. Rev. B* **86**, 115129 (2012).
- [9] Yuval Oreg and David Goldhaber-Gordon, “Two-channel kondo effect in a modified single electron transistor,” *Phys. Rev. Lett.* **90**, 136602 (2003).
- [10] RM Potok, IG Rau, Hadas Shtrikman, Yuval Oreg, and D Goldhaber-Gordon, “Observation of the two-channel kondo effect,” *Nature* **446**, 167–171 (2007).
- [11] Z Iftikhar, Sébastien Jezouin, A Anthore, U Gennser, FD Parmentier, A Cavanna, and F Pierre, “Two-channel kondo effect and renormalization flow with macroscopic quantum charge states,” *Nature* **526**, 233 (2015).
- [12] Z Iftikhar, A Anthore, AK Mitchell, FD Parmentier, U Gennser, A Ouerghi, A Cavanna, C Mora, P Simon, and F Pierre, “Tunable quantum criticality and superballistic transport in a “charge” kondo circuit,” *Science* **360**, 5592 (2018).
- [13] K. A. Matveev, “Quantum fluctuations of the charge of a metal particle under the coulomb blockade conditions,” *Sov. Phys. JETP* **72**, 892–899 (1991).
- [14] KA Matveev, “Coulomb blockade at almost perfect transmission,” *Phys. Rev. B* **51**, 1743 (1995).
- [15] A Furusaki and KA Matveev, “Theory of strong inelastic cotunneling,” *Phys. Rev. B* **52**, 16676 (1995).
- [16] Andrew K Mitchell, LA Landau, L Fritz, and E Sela, “Universality and scaling in a charge two-channel kondo device,” *Phys. Rev. Lett.* **116**, 157202 (2016).
- [17] See Supplemental Material for further details.
- [18] Kam Tuen Law, Dmitri E Feldman, and Yuval Gefen, “Electronic mach-zehnder interferometer as a tool to probe fractional statistics,” *Phys. Rev. B* **74**, 045319 (2006).
- [19] Michael Pustilnik and Leonid Glazman, “Kondo effect in quantum dots,” *Journal of Physics: Condensed Matter* **16**, R513 (2004).
- [20] M Pustilnik and LI Glazman, “Kondo effect induced by a magnetic field,” *Phys. Rev. B* **64**, 045328 (2001).
- [21] Eran Sela and Ian Affleck, “Nonequilibrium critical behavior for electron tunneling through quantum dots in an aharonov-bohm circuit,” *Phys. Rev. B* **79**, 125110 (2009).
- [22] M Pustilnik, L Borda, LI Glazman, and J Von Delft, “Quantum phase transition in a two-channel-kondo quantum dot device,” *Phys. Rev. B* **69**, 115316 (2004).
- [23] HT Mebrahtu, IV Borzenets, H Zheng, Yu V Bomze, AI Smirnov, Serge Florens, HU Baranger, and G Finkelstein, “Observation of majorana quantum critical behaviour in a resonant level coupled to a dissipative environment,” *Nat. Phys.* **9**, 732 (2013).
- [24] AJ Keller, L Peeters, CP Moca, Ireneusz Weymann, Diana Mahalu, V Umansky, G Zaránd, and D Goldhaber-Gordon, “Universal fermi liquid crossover and quantum criticality in a mesoscopic system,” *Nature* **526**, 237–240 (2015).
- [25] Andrew K Mitchell, Eran Sela, and David E Logan, “Two-channel kondo physics in two-impurity kondo models,” *Phys. Rev. Lett.* **108**, 086405 (2012).
- [26] Eran Sela and Yuval Oreg, “Adiabatic pumping in interacting systems,” *Phys. Rev. Lett.* **96**, 166802 (2006).
- [27] Eran Sela, Andrew K Mitchell, and Lars Fritz, “Exact crossover green function in the two-channel and two-impurity kondo models,” *Phys. Rev. Lett.* **106**, 147202 (2011).
- [28] Andrew K Mitchell and Eran Sela, “Universal low-temperature crossover in two-channel kondo models,” *Phys. Rev. B* **85**, 235127 (2012).
- [29] Eran Sela and Andrew K Mitchell, “Local magnetization in the boundary ising chain at finite temperature,” *Jour. Stat. Mech.* **2012**, P04006 (2012).
- [30] R Chatterjee and A Zamolodchikov, “Local magnetization in critical ising model with boundary magnetic field,” *Mod. Phys. Lett. A* **9**, 2227–2234 (1994).
- [31] Winston Pouse, Lucas Peeters, Connie L Hsueh, Ulf Gennser, Antonella Cavanna, Marc A Kastner, Andrew K Mitchell, and David Goldhaber-Gordon, “Quantum simulation of an exotic quantum critical point in a two-site charge kondo circuit,” *Nature Physics* , 1–8

(2023).

- [32] Deepak B. Karki, Edouard Boulat, and Christophe Mora, “Double-charge quantum island in the quasibalistic regime,” *Phys. Rev. B* **105**, 245418 (2022).
- [33] Pedro LS Lopes, Ian Affleck, and Eran Sela, “Anyons in multichannel kondo systems,” *Phys. Rev. B* **101**, 085141 (2020).

- [34] Yashar Komijani, “Isolating kondo anyons for topological quantum computation,” *Phys. Rev. B* **101**, 235131 (2020).
- [35] Dor Gabay, Cheolhee Han, Pedro L. S. Lopes, Ian Affleck, and Eran Sela, “Multi-impurity chiral kondo model: Correlation functions and anyon fusion rules,” *Phys. Rev. B* **105**, 035151 (2022).
- [36] Matan Lotem, Eran Sela, and Moshe Goldstein, “Manipulating non-abelian anyons in a chiral multi-channel kondo model,” arXiv preprint arXiv:2205.04418 (2022).

## SUPPLEMENTARY INFORMATION: CALCULATION OF THE CURRENT

We write the tunneling Hamiltonian  $H_T = T_1 + T_2$ ,  $T_1 = \lambda_1 \psi_0^\dagger(-L) \psi_1(-L) e^{iV/t} e^{i\phi} + h.c.$ , and  $T_2 = \lambda_2 \psi_0^\dagger(L) \psi_1(L) e^{iV/t} + h.c.$ . We set  $e = \hbar = v_F = 1$ . We obtain the current operator

$$\begin{aligned} I &= \frac{dN_0}{dt} = i[H, N_0] = I_1 + I_2, \\ I_1 &= -i\lambda_1 \psi_0^\dagger(-L) \psi_1(-L) e^{iV/t} e^{i\phi} + h.c. \\ I_2 &= -i\lambda_2 \psi_0^\dagger(L) \psi_1(L) e^{i\phi} + h.c. \end{aligned} \quad (12)$$

where  $N_0 = \int dx \psi_0^\dagger \psi_0$  and  $\{\psi_i(x), \psi_{i'}(x')\} = \delta_{ii'} \delta(x - x')$ . We evaluate the current

$$\langle I(t=0) \rangle = -i \int_{-\infty}^0 dt \langle 0 | [I(0), H_T(t)] | 0 \rangle = I_0 + I_\Phi, \quad (13)$$

where  $I_0$  does not depend on  $\phi$  and  $I_\Phi$  contains terms proportional to  $e^{-i\phi}$ . For  $I_0$  one finds

$$\begin{aligned} I_0 &= -|\lambda_1|^2 \int_{-\infty}^{\infty} dt e^{iVt} (\langle \psi_0^\dagger(-L) \psi_0(-L, t) \rangle \langle \psi_1(-L) \psi_1^\dagger(-L, t) \rangle - \langle \psi_0(-L, t) \psi_0^\dagger(-L) \rangle \langle \psi_1^\dagger(-L, t) \psi_1(-L) \rangle) \\ &\quad + (\lambda_1 \rightarrow \lambda_2, -L \rightarrow L). \end{aligned} \quad (14)$$

For the free propagators we have

$$\langle \psi_i(x, t) \psi_j^\dagger \rangle = \langle \psi_j^\dagger(x, t) \psi_i \rangle = \frac{\delta_{ij}}{2\pi} \frac{1}{\delta + i(t-x)}, \quad (15)$$

which gives

$$I_0 = -(|\lambda_1|^2 + |\lambda_2|^2) \int_{-\infty}^{\infty} dt e^{iVt} \left( \frac{1}{(\delta - it)^2} - \frac{1}{(\delta + it)^2} \right) = \frac{V}{2\pi} (|\lambda_1|^2 + |\lambda_2|^2). \quad (16)$$

Using the Landauer formula, we associate reflection coefficients

$$R_i = |\lambda_i|^2, \quad (i = 1, 2). \quad (17)$$

Reinserting units, this corresponds to a conductance of  $\frac{I_0}{V} = \frac{e^2}{h} (|\lambda_1|^2 + |\lambda_2|^2)$ , and  $R_i = |\frac{\lambda_i}{\hbar v_F}|^2$ ,  $(i = 1, 2)$ .

For the interference term we have

$$I_\Phi = \lambda_1 \lambda_2^* e^{i\phi} \int_{-\infty}^{\infty} dt e^{iVt} (\langle \psi_0^\dagger(-L) \psi_0(+L, t) \rangle \langle \psi_1(-L) \psi_1^\dagger(+L, t) \rangle - \langle \psi_0(+L, t) \psi_0^\dagger(-L) \rangle \langle \psi_1^\dagger(+L, t) \psi_1(-L) \rangle) + h.c. \quad (18)$$

In the absence of a QD along the path between  $x = -L$  to  $x = L$  in channel 1, we obtain Eq. (4) of the main text,

$$I_\Phi = -\lambda_1 \lambda_2^* e^{i\phi} e^{iV2L} \int_{-\infty}^{\infty} dt e^{iVt} \left( \frac{1}{(\delta - i(t+2L))^2} - \frac{1}{(\delta + i(t+2L))^2} \right) = \frac{V}{2\pi} (\lambda_1 \lambda_2^* e^{i\phi} + h.c.). \quad (19)$$

Eventually,

$$I = I_0 + I_\Phi = \frac{V}{2\pi} |\lambda_1 + \lambda_2 e^{i\phi}|^2. \quad (20)$$

Eq. (19) can be applied for the general case with a scattering of arm 1 through the QD. The frequency space,  $G(\omega, -L, L) = G_0(\omega, -L, L) + G_0(\omega, -L, 0)\mathcal{T}(\omega)G_0(\omega, 0, L)$ , translates simply to  $G(\omega, -L, L) = G_0(\omega, -L, L)\mathcal{S}(\omega)$ . Eq. (19) gives the current as the Fourier transform of the product of correlators. We see that the Fourier transform changes by the extra factor  $\mathcal{S}(\omega)$  evaluated at  $\omega = V$ . It contains both an absolute value, dictating the visibility, and a phase.